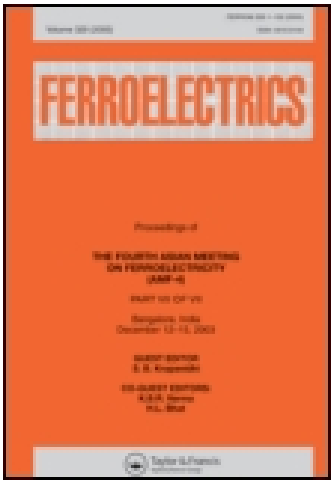

Ferroelectrics
Publication details, including instructions for authors and subscription information:
http://www.tandfonline.com/loi/gfer20

Preparation and Characterization of Mn-Doped $(Ba_{0.85}Ca_{0.15})(Zr_{0.1}Ti_{0.9})O_3$ Ceramics

A. Di Loreto[ab], A. Frattini[ab], R. Machado[b], O. de Sanctis[b] & M. G. Stachiotti[b]

[a] Área Física, Dpto. de Química Física, FCByF, Universidad Nacional de Rosario, Argentina

[b] Instituto de Física Rosario, Universidad Nacional de Rosario, Argentina

Published online: 02 May 2014.

To cite this article: A. Di Loreto, A. Frattini, R. Machado, O. de Sanctis & M. G. Stachiotti (2014) Preparation and Characterization of Mn-Doped $(Ba_{0.85}Ca_{0.15})(Zr_{0.1}Ti_{0.9})O_3$ Ceramics, Ferroelectrics, 463:1, 105-113, DOI: 10.1080/00150193.2014.892376

To link to this article: http://dx.doi.org/10.1080/00150193.2014.892376

Ferroelectrics, 463:105–113, 2014

ISSN: 0015-0193 print / 1563-5112 online
DOI: 10.1080/00150193.2014.892376

Taylor & Francis
Taylor & Francis Group

Preparation and Characterization of Mn-Doped $(Ba_{0.85}Ca_{0.15})(Zr_{0.1}Ti_{0.9})O_3$ Ceramics

A. DI LORETO,[1,2] A. FRATTINI,[1,2] R. MACHADO,[2]
O. DE SANCTIS,[2] AND M. G. STACHIOTTI[2,*]

[1]Área Física, Dpto. de Química Física, FCByF, Universidad Nacional de Rosario, Argentina
[2]Instituto de Física Rosario, Universidad Nacional de Rosario, Argentina

MnO_2-doped lead free 0.5[Ba($Zr_{0.2}Ti_{0.8}$)O_3]-0.5[($Ba_{0.7}Ca_{0.3}$)TiO_3] ceramics were synthesized by a high-energy ball milling process. We studied the phase formation process along different steps of the mechanical milling. We show that the addition of a small amount of MnO_2 (x < 0.5 mol.%) improves the dielectric and ferroelectric properties of the ceramics. It is found that the doping with manganese increases the dielectric constant and reduces the loss, which decreases considerably as the Mn content increases. The remnant polarization of the doped ceramics is increased by 10%.

Keywords Lead-free piezoelectrics; BCZT

Introduction

In recent years, especially after the publication of grain-oriented $Na_{0.5}K_{0.5}NbO_3$-based ceramics [1], the researches on lead-free piezoelectric ceramics have got much progress [2–6]. The enhancement of the electromechanical response in those materials is achieved by compositional engineering, where the composition of a solid-solution is optimized by bringing the material to the proximity of a structural instability, such as a morphotropic phase boundary (MPB). For example, the newly discovered lead-free $(1-x)Ba(Ti_{0.8}Zr_{0.2})O_3 - x(Ba_{0.7}Ca_{0.3})TiO_3$ (BCZT) ceramic system by Liu and Ren [7] presents a phase diagram similar to that of PZT showing a MPB starting from a tricritical triple point of a cubic paraelectric phase, ferroelectric rhombohedral, and tetragonal phases. During the last years, BCZT ceramics have attracted great attention due to their excellent piezoelectric properties [6–13], particularly for the composition $x = 0.5$ whose longitudinal piezoelectric coefficient d_{33} is reported to be over 600 pC/N. High d_{33} values are obtained for ceramics processed at very high calcination (1350°C) and sintering (1500°C) temperatures, while the Curie temperature is just only about 90°C [14], which limits the practical use. Therefore, it is necessary to lower the processing temperatures of the ceramics and to increase the Curie temperature.

Received September 2, 2013; in final form October 18, 2013.
*Corresponding author. E-mail: stachiotti@ifir-conicet.gov.ar
Color versions of one or more of the figures in the article can be found online at www.tandfonline.com/gfer.

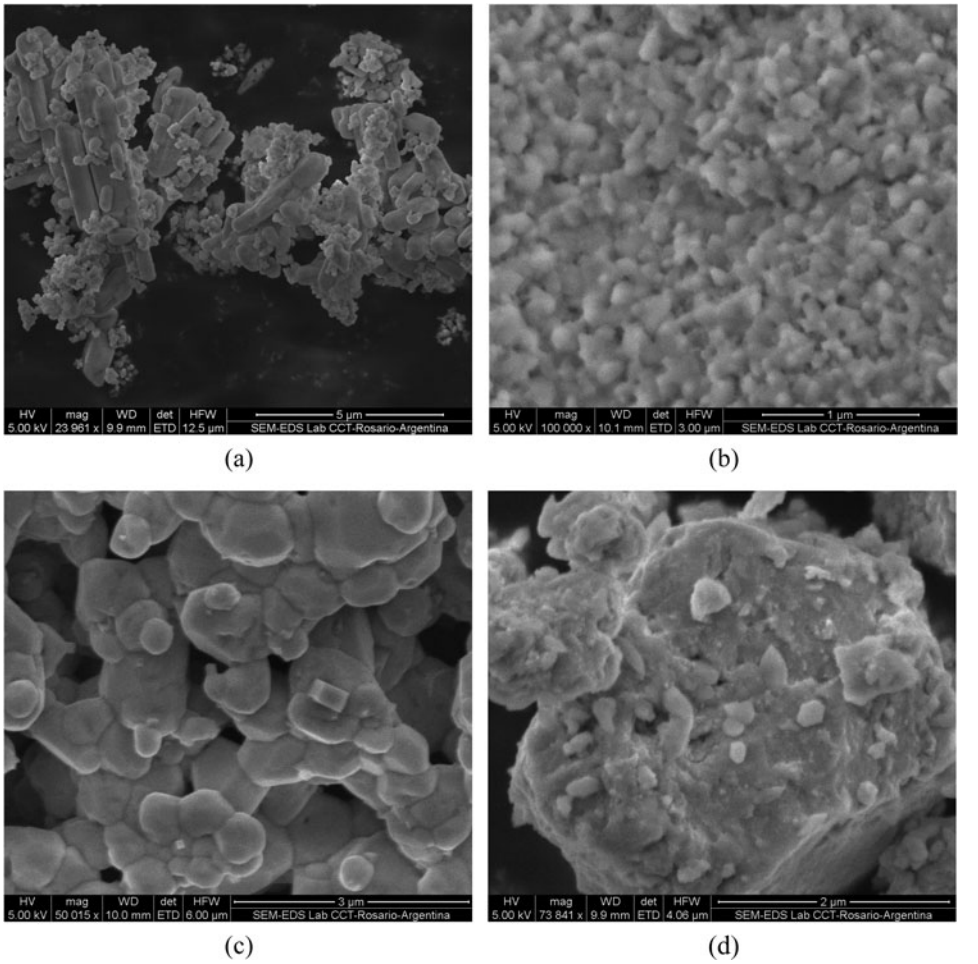

Figure 1. SEM images of un-milled $BaCO_3$, $CaCO_3$, TiO_2 and ZrO_2 powders (a), milled for 24 h. (b), after calcination (c), and milled for 24 h after calcination (d).

The performances of ferroelectric ceramics are closely related to the ways they are processed. In general, the conventional solid state reaction method requires high calcination and sintering temperatures, resulting in the loss of volatile components, thus worsening the microstructural and subsequently the electrical properties. High energy mechanochemical milling process has been shown to enable that some ferroelectric materials can be synthesized directly from their oxide precursors in the form of nano-sized powders, without the need for the calcination at intermediate temperatures, thus making the process very simple and cost-effective [15]. Another way to improve properties of specific ceramics is by doping, which is a very important and widely accepted technique. For example, it has been reported that BCZT base compositions modified with ZnO [16] and CeO_2 [17] showed improved properties. In this work we synthesized BCZT ceramics by a high-energy ball milling process, studying the phase formation process along different steps of the mechanical milling. We also investigated the effect of adding different amounts of MnO_2 on the dielectric and ferroelectric properties.

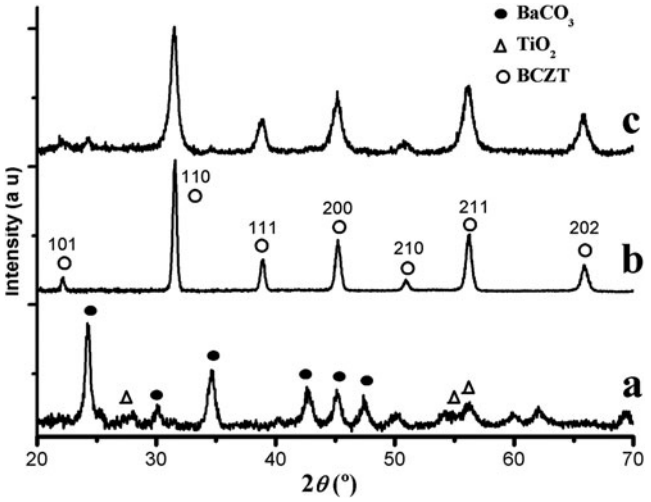

Figure 2. XRD patterns of $BaCO_3$, $CaCO_3$, TiO_2 and ZrO_2 powders milled for 24 h. (a) , after calcination (b), and milled for 24 h after calcination (c).

Experimental

$0.5[Ba(Zr_{0.2}Ti_{0.8})O_3]$-$0.5[(Ba_{0.7}Ca_{0.3})TiO_3]$ powders were synthesized from a mixture of $BaCO_3$, $CaCO_3$, TiO_2 and ZrO_2 by a high-energy milling process using a planetary ball mill equipment (Torrey Hills Technologies ND 0.4 L). The precursor powders were weighed based on the stoichiometric formula and milled for 24 h at 700 rpm. The milled powder was calcined at 1250°C for 4 h. Manganese dioxide (MnO_2) was then added to the calcined powder at concentrations ranging between 0 and 1 mol.%. The resulting powders were ball milled again for 24 h. The whole ball milling process was done in dry conditions, i.e. without the addition of a solvent in the milling jar. The obtained powders were pressed

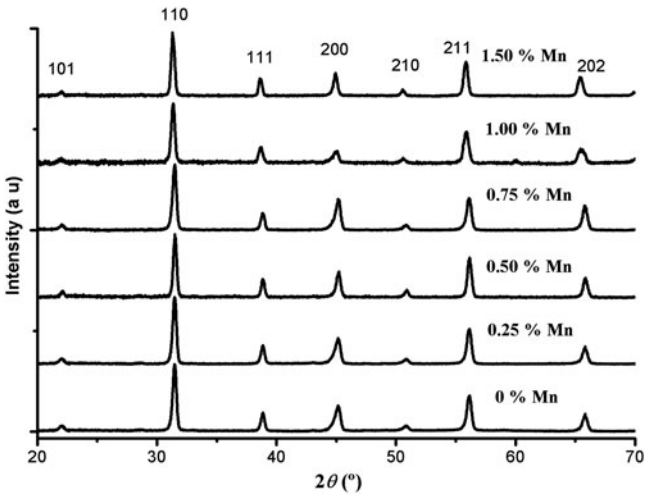

Figure 3. XRD patterns of undoped and Mn-doped BCZT ceramics.

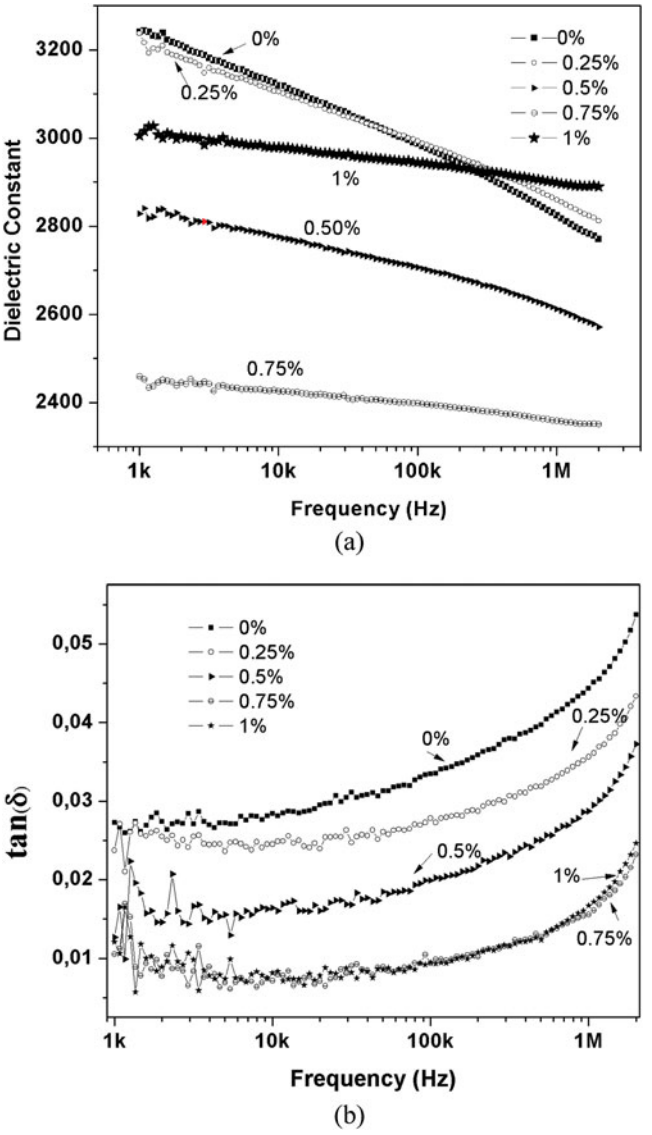

Figure 4. Frequency dependence of dielectric constant (top panel) and loss (bottom panel) of undoped and Mn-doped BCZT ceramics measured at 17°C.

into disc-shape pellets 10 mm in diameter. The pellets were sintered at 1500°C for 3 h. Crystal structure was analyzed by X-ray diffraction (XRD) using a Philips X'Pert Pro X-ray diffractometer. The microstructure was observed by scanning electron microscopy (SEM) using a FEI Quanta 200 FESEM Environmental. For electrical studies, silver electrodes were sputtered on both sides of the samples. The temperature dependence of the dielectric properties of the ceramics was measured from 1 kHz to 2 MHz using an LCR meter (QuadTech 7600 plus) attached to a programmable furnace. The hysteresis loops were measured at room temperature using a Sawyer-Tower circuit.

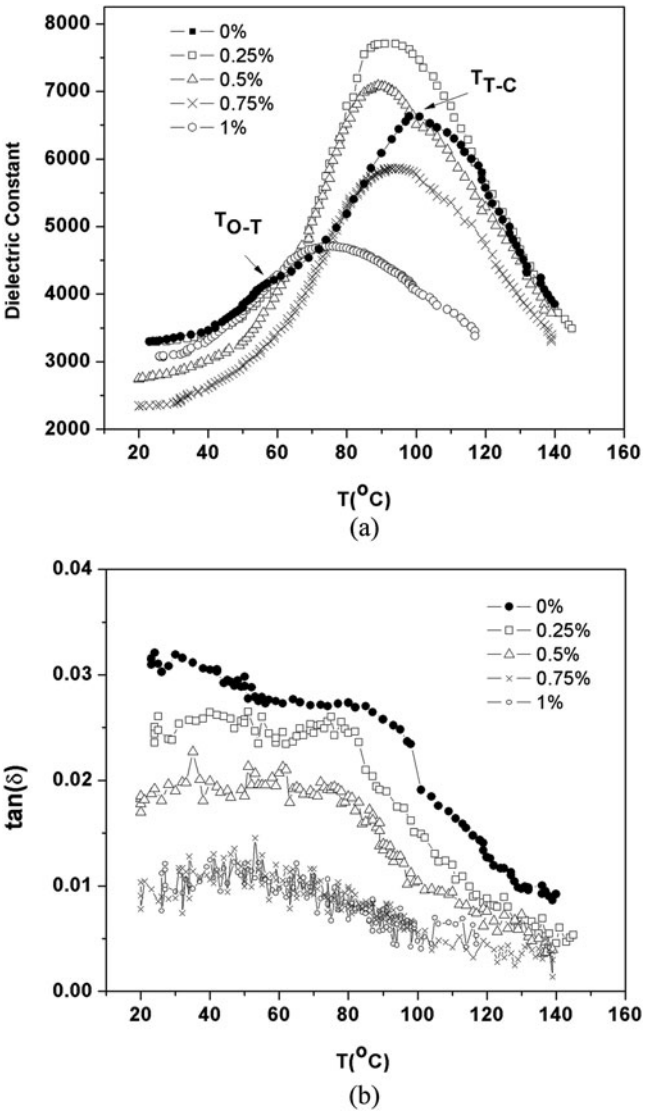

Figure 5. Temperature dependence of the dielectric constant (top panel) and loss (bottom panel) of the Mn-doped BCTZ ceramics measured at 100 kHz.

Results and Conclusions

Figures 1 and 2 show SEM images and XRD patterns of powders (with no addition of MnO_2) along the mechanical milling procedure. The un-milled mixture is characterized by sharp diffraction peaks due to the starting $BaCO_3$, $CaCO_3$, TiO_2 and ZrO_2 powders because of their good crystallinity and large particle size. Fig. 1(a) shows a panoramic view of the starting powders, where elongated $BaCO_3$ particles (length ≈ 3 μm) coexist with more isotropic oxide particles of smaller size. Fig. 1(b) shows that, after milling for 24 h, the particles have a smaller and more homogeneous size. This refinement in particle size is also reflected from the XRD patterns, where the diffraction peaks were greatly broadened

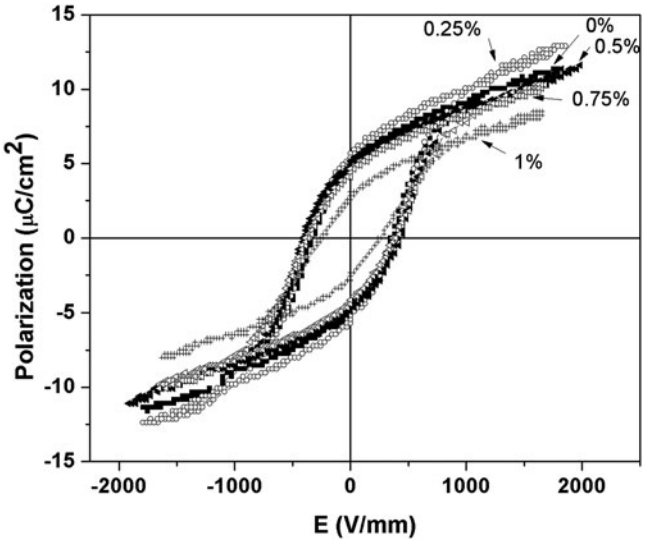

Figure 6. P–E hysteresis loops of the Mn-doped BCTZ ceramics measured at 50 Hz.

and reduced (Fig. 2(a)), compared with the one of the un-milled sample. We note that the XRD pattern of the 24 h-milled powder shown in Fig. 2(a) shows no signature of peaks corresponding to the perovskite BCZT structure. This seems to be a general feature in the mechanochemical reaction mechanism of carbonate-oxide mixtures, where an amorphous carbonate complex is formed which only decomposes after a very prolonged milling time [18]. After calcination at 1250°C, single phase BCZT with a well-developed XRD pattern is obtained (Figure 2(b)). A SEM image of the calcined powders is presented in Figure 1(c), which shows BCZT particles bonded by sintering necks. After milling for 24 h, the diffraction peaks were greatly broadened and reduced (Fig. 2(c)) indicating that the milling has a great effect in the refinement of particle size, breaking the sintering necks (Fig. 1(d)).

To investigate the effects of MnO_2 as sintering aids, different amounts of this oxide were added (with concentrations ranging between 0 and 1 mol.%) to the calcinated powders. Subsequently the batch of samples was ball milled for 24 h and pressed into disc-shape pellets. Fig. 3 shows the XRD patterns of the undoped and Mn-doped BCZT ceramics sintered at 1500°C. It can be seen that a single perovskite phase has been obtained in all the samples. Since no secondary phases were observed in Mn-doped pellets, it is concluded that Mn might go into the lattice of the perovskite structure.

Figure 4 gives the frequency dependence of dielectric constant (K) and loss tangent ($\tan\delta$) measured at 17°C. It can be seen in the left panel of the figure that there is practically no difference between the pure sample and the one doped with 0.25%, while K decreases considerably at higher doping. We note however that the 1% doped sample displays a strong increment of K. It is interesting to remark that the addition of MnO_2 reduces considerably the frequency dispersion of the dielectric constant and the dielectric loss (right panel of Fig. 4). These results indicate that the addition of Mn restrains the concentration of oxygen vacancies; a possible mechanism could be that manganese ions promote the oxidation of Ti^{+3} ions ($Mn^{+4} + Ti^{+3} \rightarrow Mn^{+3} + Ti^{+4}$). A similar improvement in the dielectric loss due to Mn doping was observed in BZT ceramics [19].

Figure 5 shows the temperature dependent values of dielectric constant at 100 kHz measured on heating (left panel), and the corresponding loss (right panel). The undoped

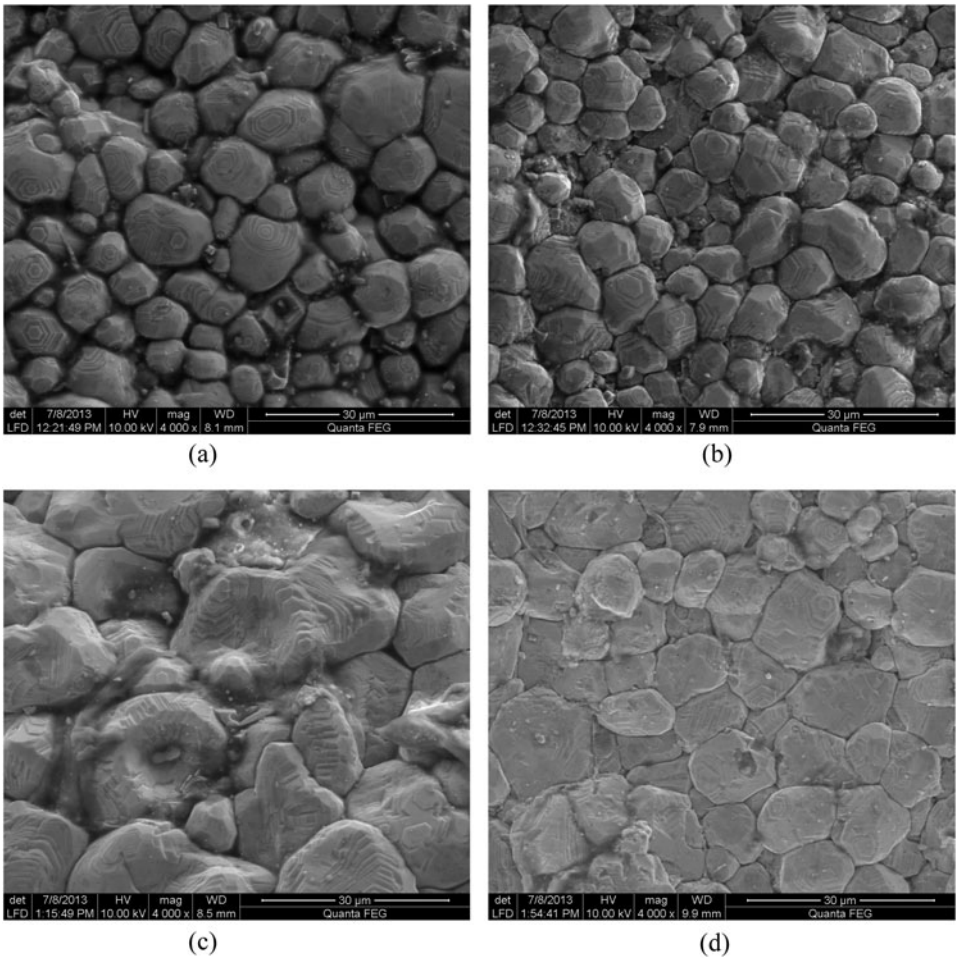

Figure 7. SEM images of Mn-doped BCZT ceramics. (a) undoped, (b) 0.25%, (c) 0.5%, (d) 0.75%.

BCZT system exhibits two phase transition peaks: the first is associated with the O-T phase transition near 54°C on heating, (40°C on cooling, not shown here), while the second with the T-C phase transition at 100°C on heating (83°C on cooling). The dielectric constant reaches a value of approximately 6700 at $T_{\text{T-C}}$. The addition of MnO_2 reduces the Curie temperature and produces that the O-T phase transition peak becomes less noticeable. The sample doped with 0.25% Mn displays however a transition peak at $T_{\text{T-C}}$ much more noticeable ($K = 7700$). When the Mn content further increases, the transition peak gradually widens. As seen in the right panel of Fig. 5, the addition of Mn reduces the dielectric loss considerably in the entire temperature range.

The polarization hysteresis curves of the samples are shown in Fig. 6. All the curves showed saturation polarization when an electric field of ∼2 kV/mm was applied. The undoped ceramic presents a remnant polarization of 5 μC/cm^2 and coercive field of 365 V/mm, approximately. The addition of a small amount of manganese (0.25%) increases the remnant polarization by 10% and the coercive field to 392 V/mm. The hysteresis loops of the samples doped with 0.5% and 0.75% Mn are practically similar to the one of the pure

sample, while a greater incorporation of MnO_2 produces a noticeable worsening of the ferroelectric properties of the ceramics. The 1% doped sample displays a remnant polarization of 2.7 μC/cm^2 and coercive field of 275 V/mm.

The electrical properties presented above can be understood from the effect of Mn ions on the microstructure of the ceramics. Fig. 7 shows SEM images of the un-doped (a), 0.25% (b), 0.5% (c) and 0.75% (d) doped BCZT ceramics. It is clear from the figures that the addition of small amounts of MnO_2 (0.25% and 0.5%) favors grain coalescence, which promotes grain growth. However, the excess of MnO_2 ($x > 0.5\%$) produces the suppression of grain growth (see Fig. 7(d)). A possible explanation could be the following: if the Mn concentration exceeds the solubility limit, the excess of Mn ions may accumulate at the grain boundaries, preventing grain growth [20].

In conclusion, we have prepared BCZT ceramics by a high-energy ball milling process, studying the phase formation process along different steps of the mechanical milling. We investigated the effect of adding different amounts of MnO_2 on the dielectric and ferroelectric properties of the ceramics. We showed that the addition of a small amount of MnO_2 (<0.5 mol.%) decreases the diffuseness of the T–C phase transition and improves the ferroelectric properties of the ceramics. The dielectric loss of the Mn-doped BCZT ceramics is lower than that of the undoped samples, and decreases considerably as the Mn content increases.

Funding

This work was sponsored by Consejo Nacional de Investigaciones Científicas y Tecnológicas (CONICET) and Agencia Nacional de Promoción Científica y Tecnológica (ANPCyT) de la República Argentina. MGS thanks for the support from Consejo de Investigaciones de la Universidad Nacional de Rosario (CIUNR).

References

1. Y. Saito, H. Takao, T. Tani, T. Nonoyama, K. Takatori, T. Homma, T. Nagaya, and M. Nakamura, Lead-free piezoceramics. *Nature*. **432**, 84–87 (2004).
2. M. Maerder, D. Damjanovic, and N. Setter, Lead Free Piezoelectric Materials. *J Electroceram*. **13**, 385–392 (2004).
3. T. Takenaka, and H. Nagata, Current status and prospects of lead-free piezoelectric ceramics. *J Eur Ceram Soc*. **25**, 2693–2700 (2005).
4. P. K. Panda, Review: environmental friendly lead-free piezoelectric materials. *J Mater Sci*. **44**, 5049–5062 (2009).
5. Y. Q. Lu, and Y. X. Li, A review on lead-free piezoelectric ceramics studies in china. *J Adv Dielectr.* **1**, 269–288 (2011).
6. S. O. Leontsev, and R. E. Eitel, Progress in engineering high strain lead-free piezoelectric ceramics. *Sci Technol Adv Mater*. **11**, 044302-1-13 (2010).
7. W. Liu, and X. Ren, Large Piezoelectric Effect in Pb-Free Ceramics. *Phys Rev Lett*. **103**, 257602-1-4 (2009).
8. W. Li, Z. Xu, R. Chu, P. Fu, and G. Zang, You have full text access to this content Piezoelectric and Dielectric Properties of $(Ba_{1-x}Ca_x)(Ti_{0.95}Zr_{0.05})O_3$ Lead-Free Ceramics *J Am Ceram Soc*. **93**, 2942–2944 (2010).
9. M. Porta, T. Lookman, and A. Saxena, Effects of criticality and disorder on piezoelectric properties of ferroelectrics. *J Phys: Condens Matter*. **22**, 345902-1-14 (2010).
10. W. Li, Z. Xu, R. Chu, P. Fu, and G. Zang, High piezoelectric d_{33} coefficient in $(Ba_{1-x}Ca_x)(Ti_{0.98}Zr_{0.02})O_3$ lead-free ceramics with relative high Curie temperature. *Mater Lett*. **64**, 2325–2327 (2010).

11. W. Li, Z. Xu, R. Chu, P. Fu, and G. Zang, Polymorphic phase transition and piezoelectric properties of $(Ba_{1-x}Ca_x)(Ti_{0.9}Zr_{0.1})O_3$ lead-free ceramics. *Physica B*. **405**, 4513–4516 (2010).
12. S. W. Zhang, H. L. Zhang, B. P. Zhang, and S. Yang, Phase-transition behavior and piezoelectric properties of lead-free $(Ba_{0.95}Ca_{0.05})(Ti_{1-x}Zr_x)O_3$ ceramics. *J Alloy Compd*. **506**, 131–135 (2010).
13. D. Damjanovic, A. Biancoli, L. Batooli, A. Vahabzadeh, and J. Trodahl, Elastic, dielectric, and piezoelectric anomalies and Raman spectroscopy of $0.5Ba(Ti_{0.8}Zr_{0.2})O_3$-$0.5(Ba_{0.7}Ca_{0.3})TiO_3$. *Appl Phys Lett*. **100**, 192907-1-4 (2012).
14. P. Wang, X. Y. Li, and Y. Q. Lu, Enhanced piezoelectric properties of $(Ba_{0.85}Ca_{0.15})$ $(Ti_{0.9}Zr_{0.1})O_3$ lead-free ceramics by optimizing calcination and sintering temperature. *J Eur Ceram Soc*. **31**, 2005–2012 (2011).
15. L. B. Kong, T. S. Zhang, J. Ma, and F. Boey, Progress in synthesis of ferroelectric ceramic materials via high-energy mechanochemical technique. *Progress Mat Sci*. **53**, 207–322 (2008).
16. J. G. Wu, D. Q. Xiao, W. J. Wu, Q. Chen, J. G. Zhu, Z. C. Yang, and J. Wang, Role of room-temperature phase transition in the electrical properties of (Ba, Ca)(Ti, Zr)O_3 ceramics. *Scrip Mater.* **65**, 771–774 (2011).
17. Y. R. Cui, X. Y. Liu, M. H. Jiang, X. Y. Zhao, X. Shan, W. H. Li, C. L. Yuan, and C. R. Zhou, Lead-free $(Ba_{0.85}Ca_{0.15})(Ti_{0.9}Zr_{0.1})O_3$–$CeO_2$ ceramics with high piezoelectric coefficient obtained by low-temperature sintering. *Ceram Int*. **38**, 4761–4764 (2012).
18. T. Rojac, M. Kosec, M. Połomska, B. Hilczer, P. Segedin, A. Bencan, Mechanochemical reaction in the K_2CO_3–Nb_2O_5 system. *J Eur Ceram Soc*. **29**, 2999–3006 (2009).
19. W. Cai, C. Fu, J. Gao, and X. Deng, Effect of Mn doping on the dielectric properties of $BaZr_{0.2}Ti_{0.8}O_3$ ceramics. *J Mater Sci: Mater Electron*. **21**, 317–325 (2010).
20. L. X. He, and C. E. Li, Effects of addition of MnO on piezoelectric properties of lead zirconate titanate. *J Mater Sci*. **35**, 2477–2480 (2000).